

Can Green Dimethyl Carbonate Synthesis be More Effective? A Catalyst Recycling Study Benefiting from Experimental Kinetics and DFT Modeling

Stéphane Chambrey,^{a,b} Mahboubeh Poor Kalhor,^c Henry Chermette^c and Danielle Ballivet-Tkatchenko^{*,a}

^aInstitut de Chimie Moléculaire de l'Université de Bourgogne, Université de Bourgogne, UMR CNRS 6302 9 Av. Alain Savary, 21000 Dijon, France

^bUnité de Catalyse et Chimie du Solide, Université Lille 1, UMR CNRS 8181 59655 Villeneuve d'Ascq cedex, France

^cInstitut des Sciences Analytiques, University of Lyon, Université Lyon 1 (UCBL) and UMR CNRS 5280, 5 rue de la Doua, 69100 Villeurbanne, France

Dibutylmetoxiestannanas são conhecidas por catalisar a reação entre dióxido de carbono e metanol, produzindo dimetil carbonato. Apesar das similaridades entre *din*-butil- e *ditert*-butildimetoxiestanana, os complexos isolados ao fim do reciclo tem características estruturais diferentes. Na série *din*-butil, um complexo decaestanho(IV) foi caracterizado e é menos ativo que o precursor estannana. Experimentos cinéticos indicam que todos os centros de estanho não são ativos, o que é confirmado quando se compara com o complexo binuclear relacionado 1,3-dimetoxitetran-butildistanoxana. Na série *ditert*-butil, o complexo triestanho(IV) isolado após o reciclo apresenta características relacionadas ao efeito estérico dos ligantes auxiliares volumosos 'Bu. A ligação de hidrogênio encontrada na estrutura SnOH...O(H)CH₃ prevê uma troca Sn-OH/Sn-OCH₃, uma etapa crucial para encerrar o ciclo catalítico. Cálculos de densidade funcional ressaltam que a troca Sn-OH/Sn-OCH₃ é endotérmica. Analisando conjuntamente, os resultados são promissores no papel dos complexos de baixa nuclearidade na síntese de dimetil carbonato.

Dibutyldimethoxystannanes are known to catalyze the reaction between carbon dioxide and methanol leading to dimethyl carbonate. Despite similarities between *din*-butyl- and *ditert*-butyldimethoxystannane, the recycled complexes have different structural features. In the *din*-butyl series, a decatin(IV) complex has been characterized and is less active than the stannane precursor. Kinetic experiments likely indicate that all the tin centers are not active, which is confirmed in comparing with the related dinuclear 1,3-dimethoxytetran-butyl-distannoxane complex. In the *ditert*-butyl series, the tritin(IV) complex isolated upon recycling features the steric effect of bulky 'Bu ancillary ligands. Interestingly enough, the SnOH...O(H)CH₃ hydrogen bonding found in the structure prefigures Sn-OH/Sn-OCH₃ interchange, a crucial step for closing the catalytic cycle. Density functional calculations highlight that the Sn-OH/Sn-OCH₃ exchange is endothermic. Taken together, the results cast a clear light on the significant role of complexes of low nuclearity for dimethyl carbonate synthesis.

Keywords: carbon dioxide, dimethyl carbonate, dibutyltin(IV) complexes, kinetics, DFT calculations

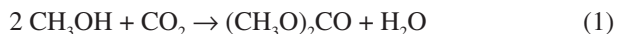
Introduction

Waste minimisation, solvent selection, atom economy, catalysis, alternative synthetic routes from sustainable resources are issues addressed in the Green Chemistry approach.¹ Accordingly, the challenge in fundamental

research is to provide tools and understanding for developing cleaner reaction pathways and products. For example, dialkyl- and diaryl carbonates are interesting targets since their conventional production involves the use of toxic phosgene or carbon monoxide rendering scale-up production problematic.² Among them, dimethyl carbonate (DMC) has low toxicity, rapid biodegradability,³ low impact on air quality,⁴ and new applications are making

*e-mail: ballivet@u-bourgogne.fr

progress in different sectors (e.g., polymers, fuels, organic synthesis).⁵ Greener processes for DMC synthesis are currently studied according to three main reaction routes: (i) carbonate transesterification, (ii) urea methanolysis, and (iii) methanol carbonation.⁶ On a stoichiometric basis, the carbonation of methanol, so-called direct synthesis of DMC, is more attractive because atom economy⁷ is highest, 83 wt.%, forming only 17 wt.% of water as the by-product (equation 1).



Moreover, equation 1 contributes to the direct fixation of carbon dioxide and, hence, to its use as renewable C1 feedstock (i.e., recycling for producing chemicals), which is one of the challenges to carbon storage for mastering anthropogenic emissions.⁸ Only a limited number of processes have thus far reached industrial stage, including production of urea, salicylic acid, organic carbonates and polycarbonates, methanol, and inorganic carbonates.⁹ Being non toxic, easy to handle, to manipulate and to store, such a C1 synthon is obviously superior to phosgene and carbon monoxide.¹⁰ However, not surprisingly, carbon dioxide is much less reactive, and its transformation into organic chemicals is better achieved with high-energy co-reactants in the presence of catalysts.

It has been reported since nearly two decades that mono- and dialkyltin(IV) complexes promote equation 1 under solventless conditions with a positive effect of CO₂ pressure,^{11,12} taking, therefore, advantage of monophasic supercritical conditions.¹³ These complexes were found to be totally selective to DMC, but they exhibit low turnover numbers (< 10). The reaction mechanism is poorly understood, justifying further studies for improvement of catalyst design and reaction conditions. We previously reported that CO₂ inserts into Sn-OR bonds of a series of *di*-butyldialkoxystannanes,¹² and stressed the role of monomeric *di*-butyldimethoxystannane for DMC formation by carrying out kinetic experiments and DFT calculations.¹⁴ Attempts to recycle the active species definitely showed an intricate network of organometallic reactions leading to polynuclear complexes, less active than the stannane precursor.^{15,16} Water is the by-product of equation 1 that accumulates in the reaction medium as DMC formation proceeds. Hence, hydrolysis of organometallic species may be at the origin of activity drop in hampering *di*-butyldimethoxystannane to be quantitatively recycled. In line with this thought, *in situ* water trapping has been shown to boost DMC conversion.¹⁷ Shifting from *n*-butyl groups as ancillary ligands to more bulky *tert*-butyl ones led to recycling different polynuclear species.¹⁸

The results herein reported provide new insight into the activity of recycled species from ¹¹⁹Bu₂Sn(OCH₃)₂ and ¹¹⁷Bu₂Sn(OCH₃)₂ on the basis of kinetics experiments and DFT calculations. On the one hand, kinetic analysis at the early stage of the reaction shows recycled high nuclearity tin species are less active than low nuclearity ones. On the other hand, DFT calculations provide the energy profile of hydroxy-methoxy ligand interchange, a key step in recycling the active species.

Results and Discussion

Kinetics experiments

The kinetics experiments were performed at high pressure (around 20 MPa) to ensure the reaction was occurring under monophasic conditions (supercritical phase) in all the cases. This was assessed by visual observation with a reactor equipped with sapphire windows as well as from fluid phase equilibria modeling.¹⁶ Importantly, monophasic conditions allowed us to run the reaction under constant volume, therefore, under known concentrations for the kinetic study. Several related dibutyltin(IV) complexes were compared aiming at identifying parameters that govern optimum recycling of the active species.

As depicted in Figure 1, ¹¹⁹Bu₂Sn(OCH₃)₂ precursor is active in DMC formation with smooth increase during 50-hour run, showing at first the reaction is not limited by thermodynamics. After depressurization of the reactor followed by workup procedure, the solid residue was reloaded into the reactor for checking the recyclability of the catalytic system. As a matter of fact, the reloaded species is less active (Figure 1).

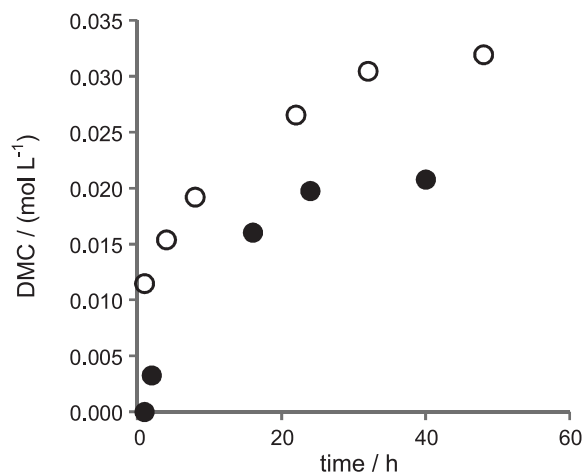
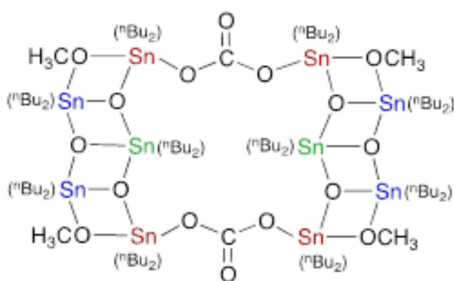


Figure 1. DMC formation with reaction time from (○) ¹¹⁹Bu₂Sn(OCH₃)₂ and (●) recycling. Reaction conditions: T = 423 K, P = 20 MPa, CH₃OH = 227 mmol, CO₂ = 400 mmol, Sn = 1.5 mmol.

Nevertheless, further recyclings (up to six) led to the same kinetic profile. Attempt to characterize the tin residue was successful. A molecular complex containing 10 tin atoms could be crystallized and characterized by single-crystal X-ray diffraction (Scheme 1).¹⁶ The structure shows two interesting features in connection with its activity. Firstly, all the tin centers bear two *n*-butyl groups, showing that the C(sp³)-Sn bonds are stable under the reaction conditions. Secondly, three different pentacoordinated tin atoms coexist, bearing oxo-, methoxy and carbonato ligands. Consequently, the lower reaction rate observed for recycled species may be ascribed to the presence of inactive tin centers.



Scheme 1. Structure of the decatin species, $({}^n\text{Bu}_2\text{SnO})_6[({}^n\text{Bu}_2\text{SnOCH}_3)_2(\text{CO}_3)]_2$; color identifies the three different tin pentacoordinations.

Determination of the partial kinetic order in tin corroborates the hypothesis. The study was performed at 411 K with initial tin concentration ranging from 0.35×10^{-2} to 10×10^{-2} mol L⁻¹. At the early stage of the reaction, DMC yield increases linearly with time, which allowed us to calculate the initial rate, r_0 , from linear regression from a significant number of online samplings for analysis according to the rate law $r_0 = (d[\text{DMC}]/dt)_0 = k[\text{Sn}]^a[\text{CO}_2]^b[\text{CH}_3\text{OH}]^c$. Pseudo zeroth-order in CO₂ and methanol concentrations applies due to their large molar excess relative to tin (> 150), thereby reducing the rate law to $r_0 = k_{\text{obs}}[\text{Sn}]^a$. The obvious advantage of the initial rate method lies in preventing rate interference of subsequent reactions, if any. The calculated tin partial order of 0.20 ± 0.05 unambiguously shows only a fraction of the tin centers play a significant role in the initial rate (Figure S1, in the Supplementary Information (SI) section).

As shown in Scheme 1, the decatin backbone arises from ${}^n\text{Bu}_2\text{Sn}(\text{IV})$ fragments being connected together via oxo, methoxy, and carbonato ligands. In order to assess the individual reactivity of such subunits, known compounds having close elemental composition were studied. Only dibutyltin(IV) complexes with the oxo and methoxy ligands have been previously isolated and characterized. The complex ${}^n\text{Bu}_2\text{SnO}$ is a commercial product, air stable, and insoluble in conventional solvents at room temperature

due to its crosslinked polymeric $({}^n\text{Bu}_2\text{SnO})_n$ structure.¹⁹ The air-sensitive 1,3-dimethoxytetrabutyl distannoxane complex, $({}^n\text{Bu}_2\text{SnOCH}_3)_2\text{O}$, is easily prepared according to conproportionation equation 2.¹⁵



The kinetic profile of these two complexes was determined at 411 K and compared with those of ${}^n\text{Bu}_2\text{Sn}(\text{OCH}_3)_2$ and the decatin species (Figure 2).

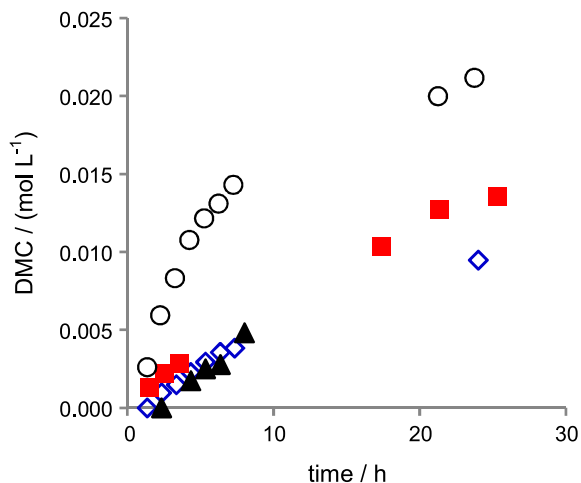


Figure 2. DMC formation with reaction time from (○) ${}^n\text{Bu}_2\text{Sn}(\text{OCH}_3)_2$, (■) $({}^n\text{Bu}_2\text{SnOCH}_3)_2\text{O}$, (◇) $({}^n\text{Bu}_2\text{SnO})_n$, and (▲) decatin. Reaction conditions: T = 411 K, P = 21 MPa, CH₃OH = 227 mmol, CO₂ = 497 mmol, Sn = 1.5 mmol.

Clearly, $\text{Bu}_2\text{Sn}(\text{OCH}_3)_2$ is by far the most active, with tin first-order,¹⁴ providing the highest initial rate with turnover frequency (TOF) of 0.096 h^{-1} . The distannoxane comes next (TOF = 0.041 h^{-1}). Tin partial order for the distannoxane was calculated to be 0.5 ± 0.05 , which strongly suggests one tin center out of two is involved in the catalytic cycle (Figure S2). Hence, the distannoxane likely disproportionates into the stannane and the oxide under the reaction conditions (the reverse of equation 2), the stannane being predominantly responsible for DMC formation. The decatin and oligomeric ${}^n\text{Bu}_2\text{SnO}$ complexes exhibit the lowest initial rate with TOFs of 0.026 and 0.022 h^{-1} , respectively, which indicates high nuclearity of the tin complex hampers DMC formation under the reaction conditions herein used. One approach to promote low nuclearity consists in tuning the steric effect of the ancillary butyl ligands. For the time being, *ditert*-butyldimethoxystannane reveals this steric effect for DMC formation.

Figure 3 reports the kinetics of DMC formation with ${}^n\text{Bu}_2\text{Sn}(\text{OCH}_3)_2$ under the same conditions as those of Figure 1. However, the recycled species is barely less active

than the stannane contrasting with the *n*-butyl case, with initial TOFs of 0.045 and 0.066 h⁻¹, respectively. Further recyclings (up to four) gave the same kinetic profile.

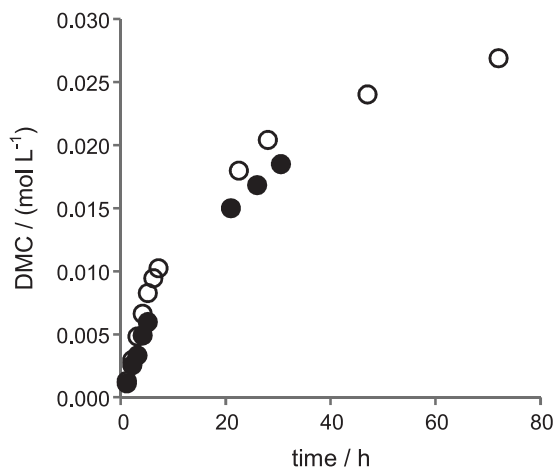
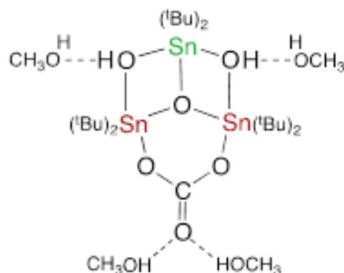


Figure 3. DMC formation with reaction time from (○) ^tBu₂Sn(OCH₃)₂ and (●) recycling. Reaction conditions: T = 423 K, P = 20 MPa, CH₃OH = 230 mmol, CO₂ = 400 mmol, Sn = 1.5 mmol.

The tin residue from recyclings was successfully characterized by single-crystal X-ray diffraction as trinuclear cluster solvated by methanol molecules (Scheme 2).¹⁸



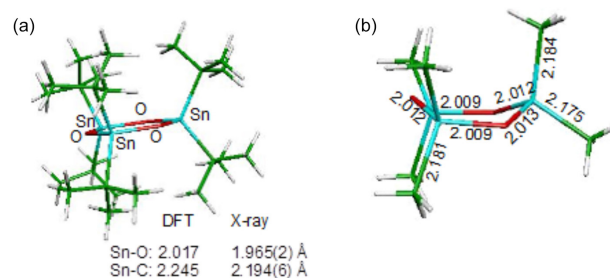
Scheme 2. Structure of the trinuclear species, [Bu₂Sn(OH)₂][Bu₂Sn(O)(CO₃)]·3CH₃OH (Sn₃-(OH)₂·3CH₃OH).

Each tin atom is pentacoordinated with two ^tBu ligands, showing the two Sn-C bonds are stable under the reaction conditions as in the ⁿBu case. In connection with DMC formation, the main feature is the presence of oxo, hydroxy, and carbonato ligands. The hydroxy ligands have formally replaced the methoxy groups of the decatin structure. Moreover, the SnOH...O(H)CH₃ hydrogen bonding characterized in the structure between hydroxy and methanol may significantly prefigures the Sn-OH/Sn-OCH₃ interchange with the concomitant formation of water. This step is crucial for closing the catalytic cycle as we have previously established that the insertion of CO₂ into Sn-OCH₃ bond to give the hemicarbonate Sn-OC(O)OCH₃ is a key elementary step to DMC.¹⁴ It was, therefore,

relevant to calculate the energetics of the Sn-OH/Sn-OCH₃ transformation as discussed in the following sub-section.

Modeling study

DFT calculations were performed at first with ^tBu₂SnO to compare the optimized structure and bond distances with those obtained from previous X-ray analysis.²⁰ The X-ray structure shows the complex crystallizes as trimer with planar 6-membered SnO ring, and the optimized calculated structure nicely fits the experimental one (Scheme 3a). In addition, the Sn-O and Sn-C bond lengths are in agreement. The effect of bulky butyl groups was further evidenced by comparing the structure of [(CH₃)₂SnO]₃ in which ^tBu groups have been replaced by methyl ones (Scheme 3b). The trimeric structure could be optimized having also tetracoordinated tin centers, but the 6-membered SnO ring is no longer planar with slightly shorter Sn-O and Sn-C bonds.

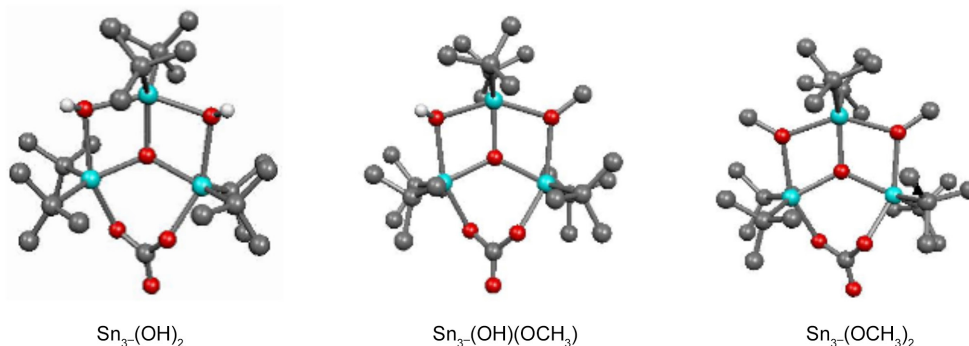


Scheme 3. Optimized structures and selected bond distances for (a) [Bu₂SnO]₃ and (b) [(CH₃)₂SnO]₃.

Nonetheless, when tin exhibits pentacoordination as in the structure depicted in Scheme 4, less steric constraint was evidenced. The corresponding optimized structure with methyl ligands, [(CH₃)₂Sn(OH)₂][(CH₃)₂Sn(O)(CO₃)]·3CH₃OH, is consistent with the X-ray structure of Sn₃-(OH)₂·3CH₃OH (Table S1).

This benchmarking study allows us to rely on the calculations of the energetics of the Sn-OH/Sn-OCH₃ exchange process with [Bu₂Sn(OR)₂][Bu₂Sn(O)(CO₃)], (R = H: Sn₃-(OH)₂; R = H, CH₃: Sn₃-(OH)(OCH₃); R = CH₃: Sn₃-(OCH₃)₂). The optimized geometries are given in Scheme 4, and relevant charges and bond lengths in Figures S1 and S2, respectively. All the structures are very similar, tin retaining its pentacoordination. No drastic differences are evidenced in charges and bond lengths (Figures S3 and S4).

The energy profile of the three compounds given in Figure 4 shows the dihydroxo species to be more stable than the mixed hydroxo-methoxy and dimethoxy ones. However, the difference is small amounting to 11.6 and 15.4 kJ mol⁻¹, respectively.



Scheme 4. Optimized structures of $[\text{Bu}_2\text{Sn(OH)}_2][(\text{Bu}_2\text{Sn})_2(\text{O})(\text{CO}_3)]$, $[\text{Bu}_2\text{Sn(OH)(OCH}_3)][(\text{Bu}_2\text{Sn})_2(\text{O})(\text{CO}_3)]$, and $[\text{Bu}_2\text{Sn(OCH}_3)_2][(\text{Bu}_2\text{Sn})_2(\text{O})(\text{CO}_3)]$. Tin (turquoise), oxygen (red), carbon (dark grey), hydrogen (light grey), hydrogen atoms of the 'Bu groups are omitted for clarity.

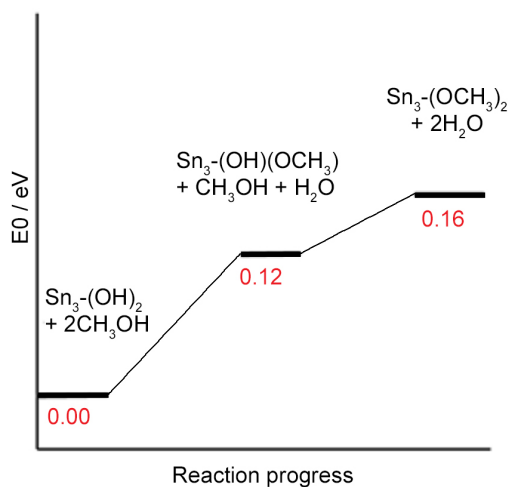


Figure 4. Energy profile of the interchange reaction between hydroxy and methoxy ligands from $[\text{Bu}_2\text{Sn(OH)}_2][(\text{Bu}_2\text{Sn})_2(\text{O})(\text{CO}_3)]$ to $[\text{Bu}_2\text{Sn(OCH}_3)_2][(\text{Bu}_2\text{Sn})_2(\text{O})(\text{CO}_3)]$.

The interchange between hydroxy and methoxy will, therefore, be driven by the experimental conditions, e.g., excess of methanol and temperature. It is worth noting that methanol solvation as observed in $\text{Sn}_3\text{-(OH)}_2 \cdot 3\text{CH}_3\text{OH}$ likely leads to lower energy. Infrared spectra also reveal methanol hydrogen bonding. The carbonato signature for $\text{Sn}_3\text{-(OH)}_2$ was calculated at 1651 ($\nu_{\text{C=O}}$) and 1130 ($\nu_{\text{C-O}}$) cm^{-1} , shifting to 1549 ($\nu_{\text{C=O}}$) and 1282 ($\nu_{\text{C-O}}$) cm^{-1} with methanol hydrogen bonding in agreement with the experimental spectrum (1549 and 1291 cm^{-1}).¹⁸

Conclusions

The dibutyltin(IV) complexes characterized during the recycling experiments from the reaction between CO_2 and methanol to afford DMC and water are polynuclear species. The kinetics of DMC formation is correlated with the nuclearity of the recycled species. The lower the nuclearity, the highest is the initial rate. DFT calculations point out tin-hydroxy fragment can be transformed into

tin-methoxy in the presence of methanol. The process being endothermic, increasing reaction temperature and methanol concentration likely promotes tin-methoxy species and thereby the concentration of active species.

Experimental

General

All manipulations were carried out under argon by using standard Schlenk tube techniques. Methanol and toluene (Carlo Erba, RPE grade) were dried and distilled from $\text{Mg(OCH}_3)_2$ and CaH_2 , respectively. Carbon dioxide N45 TP (purity 99.995%) was purchased from Air Liquide and used without further purification. ^{119}Sn was purchased from Aldrich. The other tin complexes have been synthesized and fully characterized previously in our group.^{12,15,16,18}

Kinetics experiments

Caution: when high pressures are involved, appropriate safety precautions must be taken.

In a 56 cm^3 stainless steel batch reactor equipped with magnetic stirrer bar and internal thermocouple, was introduced under argon a methanolic solution or suspension (9 cm^3) of the tin complex ($\text{Sn} = 1.5$ mmol). Then, a known mass of liquid CO_2 (ca. 20 g, 454 mmol) was transferred at room temperature with a high-pressure ISCO-260 pump, and the reactor was heated up to the desired temperature. DMC formation with time was determined by online analysis of the reaction mixture with a high-pressure sampling loop of 0.090 cm^3 . After the last sampling, the reactor was cooled down to 273 K, gently depressurized, and the liquid phase transferred for quantitative gas chromatography (GC) analysis using toluene and diethyl carbonate as internal and external standards, respectively. Comparison between these two procedures of DMC analysis gave a fit better than 3% (relative error).

GC analysis was performed on a Fisons 8000 equipped with a J&W Scientific DB-WAX 30 m capillary column and FID detector. Blank test experiments showed no DMC formation in the absence of the tin complexes.

DFT calculations

The Amsterdam Density Functional (ADF) code was herein used for all the calculations.²¹⁻²³ The PBE gradient-corrected exchange-correlation functional²⁴ and the Triple Zeta plus Polarization (TZP) basis set were retained for all the calculations, with small frozen cores. All the structures were characterized by vibrational analysis in the harmonic approximation, with no imaginary frequency for stable states.

Supplementary Information

Supplementary Information (tin order determination, selected charges and bond lengths for $\text{Sn}_3\text{-(OH)}_2$, $\text{Sn}_3\text{-(OH)(CH}_3\text{)}$ and $\text{Sn}_3\text{-(CH}_3\text{)}_2$, and selected bond lengths for $\text{Sn}_3\text{-(OH)}_2\cdot 3\text{CH}_3\text{OH}$) is available free of charge at <http://jbcbs.s bq.org.br>.

Acknowledgements

The authors gratefully acknowledge the Centre National de la Recherche Scientifique (France), the French National Agency for Research (project ANR-08-CP2D-18) for support of this work, and GENCI/CINES for HPC resources/computer time (Project cpt2130). S. C. thanks the French Ministry of Education for a PhD grant.

References

- Anastas, P. T.; Bartlett, L. B.; Kirchoff, M. M.; Williamson, T. C.; *Catal. Today* **2000**, *55*, 11.
- Delledonne, D.; Rivetti, F.; Romano, U.; *Appl. Catal., A* **2001**, *221*, 241; Uchiyama, S.; Ataka, K.; Matsuzaki, T.; *J. Organomet. Chem.* **1999**, *576*, 279.
- Rivetti, F. In *Green Chemistry*; Anastas, P. T.; Williamson, T. C., eds.; ACS Symp. Ser., 1996, 626, pp. 70.
- Katrib, Y.; Deiber, G.; Mirabel, P.; Le Calvé, S.; George, C.; Mellouki, A.; Le Bras, G.; *J. Atmos. Chem.* **2002**, *43*, 151.
- Selva, M.; Perosa, A.; *Green Chem.* **2008**, *10*, 457; Fukuoka, S.; Fukawa, I.; Tojo, M.; Oonishi, K.; Hachiya, H.; Aminaka, M.; Hasegawa, K.; Komiyama, K.; *Catal. Surv. Asia* **2010**, *14*, 146; Sakakura, T.; Kohno, K.; *Chem. Commun.* **2009**, 1312.
- Ballivet-Tkatchenko, D.; Dibenedetto, A. In *Carbon Dioxide as Chemical Feedstock*; Aresta, M., ed.; Wiley-VCH: Weinheim, Germany, 2010.
- Trost, B. M.; *Angew. Chem., Int. Ed.* **1995**, *34*, 259.
- Hunt, A. J.; Sin, E. H. K.; Marriott, R.; Clark, J. H.; *ChemSusChem* **2010**, *3*, 306; Olah, G. A.; Surya Prakash, G. K.; Goepfert, A.; *J. Am. Chem. Soc.* **2011**, *133*, 12881; Cokoja, M.; Bruckmeier, C.; Rieger, B.; Herrmann, W. A.; Kühn, F. E.; *Angew. Chem., Int. Ed.* **2011**, *50*, 8510; Markewitz, P.; Kuckshinrichs, W.; Leitner, W.; Linssen, J.; Zapp, P.; Bongartz, R.; Schreiber, A.; Müller, T. E.; *Energy Environ. Sci.* **2012**, *5*, 7281; Olajire, A. A.; *J. CO2 Util.* **2013**, *3-4*, 74.
- Behr, A.; *Chem. Eng. Technol.* **1987**, *10*, 16; Lu, X-B.; Pontzen, F.; Liebner, W.; Gronemann, V.; Rothaemela, M.; Ahlers, B.; *Catal. Today* **2011**, *171*, 242; Darensbourg, D.; *Chem. Soc. Rev.* **2012**, *41*, 1462; Aresta, M.; Dibenedetto, A.; Angelini, A.; *J. CO2 Util.* **2013**, *3-4*, 65; Maeda, C.; Miyazaki, Y.; Ema, T.; *Catal. Sci. Technol.* **2014**, *4*, 1482; Nakano, R.; Ito, S.; Nozaki, K.; *Nat. Chem.* **2014**, *6*, 325.
- Bertilsson, F.; Karlsson, H. T.; *Energy Convers. Manage.* **1996**, *37*, 1733.
- Kizlink, J.; Pastucha, I.; *Collect. Czech. Chem. Commun.* **1995**, *6*, 687; Choi, J.-C.; Sakakura, T.; Sako, T.; *J. Am. Chem. Soc.* **1999**, *121*, 3793.
- Ballivet-Tkatchenko, D.; Douteau, O.; Stutzmann, S.; *Organometallics* **2000**, *19*, 4563.
- Jessop, P. G.; Leitner, W.; *Chemical Synthesis Using Supercritical Fluids*, Wiley-VCH: Weinheim, Germany, 1999.
- Poor Kalthor, M.; Chermette, H.; Chambrey, S.; Ballivet-Tkatchenko, D.; *Phys. Chem. Chem. Phys.* **2011**, *13*, 2401.
- Ballivet-Tkatchenko, D.; Jerphagnon, T.; Ligabue, R.; Plasseraud, L.; Poinot, D.; *Appl. Catal., A* **2003**, *255*, 93.
- Ballivet-Tkatchenko, D.; Chambrey, S.; Keiski, R.; Ligabue, R.; Plasseraud, L.; Richard, P.; Turunen, H.; *Catal. Today* **2006**, *115*, 80.
- Sakakura, T.; Choi, J.-C.; Saito, Y.; Masuda, T.; Sako, T.; Oriyama, T.; *J. Org. Chem.* **1999**, *64*, 4506.
- Ballivet-Tkatchenko, D.; Burgat, R.; Chambrey, S.; Plasseraud, L.; Richard, P.; *J. Organomet. Chem.* **2006**, *691*, 1498.
- Harris, R. K.; Sebald, A.; *J. Organomet. Chem.* **1987**, *331*, C9.
- Puff, H.; Schuh, W.; Sievers, W.; Wald, W. R.; Zimmer, R.; *J. Organomet. Chem.* **1984**, *260*, 271.
- Fonseca Guerra, C.; Snijders, J. G.; te Velde, G.; Baerends, E. J.; *Theor. Chem. Acc.* **1998**, *99*, 391.
- te Velde, G. F.; Bickelhaupt, M.; van Gisbergen, S. J. A.; Fonseca Guerra, C.; Baerends, E. J.; Snijders, J. G.; Ziegler, T.; *J. Comput. Chem.* **2001**, *22*, 931.
- Baerends, E. J.; *ADF2009.01, SCM, Theoretical Chemistry*, Vrije Universiteit, Amsterdam, The Netherlands. Available at <http://www.scm.com>.
- Perdew, J. P.; Burke, K.; Ernzerhof, M.; *Phys. Rev. Lett.* **1996**, *77*, 3865.

Submitted on: September 1, 2014
Published online: October 17, 2014